ISSN No:-2456-2165 https://doi.org/10.38124/ijisrt/IJISRT24MAY1888

Design and Implementation of Multi-Node CO Air Quality Monitoring System Based on Wireless Sensor Network and Internet of Things Integrated with Solar Panel

Pillar Satya Mahardika[1]; Ainie Khuriati Riza Sulistiati[2,3]; Jatmiko Endro Suseno[2,3]*
[1]Magister of Physics, Physics Department, Faculty of Science and Mathematics,
Diponegoro University, Tembalang Campus, Semarang, Indonesia, 50275
[2]Physics Department, Faculty of Science and Mathematics,
Diponegoro University, Tembalang Campus, Semarang, Indonesia, 50275
[3]Instrumentation laboratory in, Diponegoro University, Integrated laboratory, Tembalang Campus, Semarang Indonesia, 50275

Abstract:- The increase in air pollution due to industrialization and transportation growth in developing countries raises concerns about public health impacts and financial burdens for governments. Traditional monitoring equipment is limited in deployment and real-time capabilities. This research aims to design an air quality monitoring system based on Wireless Sensor Network (WSN) and Internet of Things (IoT) integrated with solar panels. The system utilizes three sensor nodes and one sink node to monitor parameters such as temperature, humidity, and CO. Data from the sensor nodes are transmitted to the sink node via Long Range (LoRa) network, then sent to the server via WiFi for storage and online display, processed into graphs accompanied by Air Quality Index (AQI) to facilitate data analysis. Sensor calibration is conducted using standard equipment and AQMS. Calibration results show a high correlation between the sensors and standard equipment, with R^2 approaching 1 for all sensors. The system is tested in the environment of the Faculty of Science and Mathematics, Diponegoro University, and shows good average air quality results. This system is expected to contribute effectively and efficiently to maintaining and improving air quality.

Keywords:- *Wireless Sensor Network (WSN), Internet of Things (IOT), Air Quality Monitoring, Solar Panel, Long Range (Lora) Network, Real-Time Monitoring, Air Quality Index (AQI)*

I. INTRODUCTION

There is increasing public and governmental concern about air pollution in developing countries due to rapid industrialization and transportation growth. One of the most well-known effects of long-term exposure to air pollution is the significant development of respiratory diseases [1,2]. Governments may face substantial financial burdens if air quality continues to deteriorate. To prevent further air quality degradation, air quality monitoring equipment becomes an essential tool. Due to the size and cost of traditional air quality monitoring stations, they are not ideal for dense deployment in urban areas such as cities [3]. Additionally, although precise measurement results may be obtained, a highly time-consuming offline process is required. Therefore, this method cannot provide real-time data on air quality. However, high spatial and temporal resolution data on air quality is highly needed, which is the focus of this research [4].

The rapid development of Internet of Things (IoT) technology enables air quality sensing and data transmission to servers through wireless networks such as Wireless Sensor Networks (WSN) [5,6]. Currently, Wireless Sensor Networks have been widely applied in various fields such as environmental monitoring, agriculture, and the Internet of Things. In these applications, wireless communication between nodes in a Wireless Sensor Network plays a crucial role [7]. The Internet of Things has characteristics such as connectivity, intelligence, and real-time capabilities. It connects devices through wireless communication technology and endows them with sensing, computing, and decision-making abilities. This allows the Internet of Things to obtain and transmit data in real time, automate collaboration and data sharing, increase production and operational efficiency, and reduce costs.

Wireless Sensor Networks have become an important and challenging issue due to their wireless nature. WSNs can be installed and configured flexibly without the need for complex cable infrastructure. This allows for use in hard-to-reach or rapidly changing environments, such as in emergency monitoring missions. The purpose of a Wireless Sensor Network is to detect specific events or conditions in the environment. This can include fire detection, flood detection, soil moisture monitoring, and so on [8]. Research on Wireless Sensor Networks has significant implications for optimizing the use of resources, such as water or energy, by providing real-time data on usage and environmental conditions [9].

ISSN No:-2456-2165 https://doi.org/10.38124/ijisrt/IJISRT24MAY1888

The use of LoRa (Long Range) networks in WSNs (Wireless Sensor Networks) offers several advantages. LoRa can transmit data over very long distances, even up to several kilometers or more, depending on environmental conditions. This enables sensors in a WSN to communicate over large areas without requiring additional communication infrastructure. One of the main features of LoRa is its very low power consumption. Sensors in a WSN using LoRa can operate on batteries for extended periods, often years, without needing replacement. This is especially useful in applications where access to energy resources is limited or difficult [10,11].

The use of solar panels provides a sustainable and environmentally friendly power source for WSNs. By utilizing solar energy, sensors in the network can continue to operate without relying on batteries that need periodic replacement. Using solar panels as a power source can help significantly reduce air pollution. Solar panels generate electricity without the need for fossil fuels, such as coal or oil. By using solar energy to generate electricity, solar panels help reduce reliance on fossil fuel-based power plants [12]. By reducing dependence on conventional power plants, which often produce local air pollutants such as sulfur dioxide (SO2), nitrogen dioxide (NO_2), and particulate matter, solar panels help reduce local air pollution. This can provide direct health benefits to communities around areas using solar panels [13].

In previous research conducted by N. Salman, Andrew H., A. Khan, and C. J. Noakes (2019), an Indoor Air Quality Monitoring Tool Based on Wireless Sensor Network was developed. This tool used three modules, each capable of monitoring CO_2 and temperature indoors using WSN methods and projecting it into a variogram form. It used Sensirion SCD 30, Sensirion RH and temperature sensors, communication via XBee, data processing using MBED LPC 1768, and power from a 10,000 mAh battery with charging via a charger [14].

According to the regulation of the Minister of Environment and Forestry of the Republic of Indonesia Number P.14/MENLHK/SETJEN/KUM.1/7/2020 on the Standard Air Pollution Index (ISPU), Article 2 paragraph 2 stipulates that ISPU parameters include PM (Particulate Matter) 10, PM2.5, CO, NO_2, SO_2, O_3, and HC. In addition to the parameters stipulated in the regulation of the Minister of Environment and Forestry of the Republic of Indonesia Number P.14/MENLHK/SETJEN/KUM.1/7/2020 on the Standard Air Pollution Index (ISPU), there are other parameters such as temperature, humidity, and CH that are closely related to air pollution.

In the context of the article described earlier, the importance of monitoring air pollution parameters demands the existence of devices capable of simultaneously measuring various parameters. Such a device becomes essential to provide a comprehensive understanding of the air quality in a region. With the ability to perform multi-point measurements and integrated with solar panels as the power source, this tool not only allows for a more comprehensive evaluation of air pollution levels but also supports early warning efforts, crisis management, and in-depth scientific research on health and environmental impacts.

Thus, the existence of a multi-point monitoring device integrated with solar panels becomes a critical aspect in efforts to maintain and improve air quality effectively and efficiently. Therefore, a study titled “Design and Development of Multi-Node Air Quality Monitoring Based on Wireless Sensor Network and Internet of Things Integrated with Solar Panel” will be conducted.

II. RESEARCH METHODS

The hardware design for the MultiNode air quality monitoring system based on Wireless Sensor Network integrated with solar panel is divided into two parts: the hardware design of the Sensor Node and the hardware design of the Sink Node.

In the Sensor Node hardware design, the focus is on reading parameter values and communication. The parameters to be read by the Sensor Node are temperature, humidity, and CO. To read these parameters, the Sensor Node requires additional components: the DHT22 sensor for temperature and humidity readings, and the MQ-9 sensor for CO readings. The microcontroller used is the Arduino Nano, and for communication in the LoRa network, the LoRa Ra-02 module is employed. Power to operate the Sensor Node is provided by the solar panel, and a battery is used to store power from the solar panel. To clarify the block diagram of the Sensor Node hardware design, please refer to Figure 1.

ISSN No:-2456-2165 https://doi.org/10.38124/ijisrt/IJISRT24MAY1888

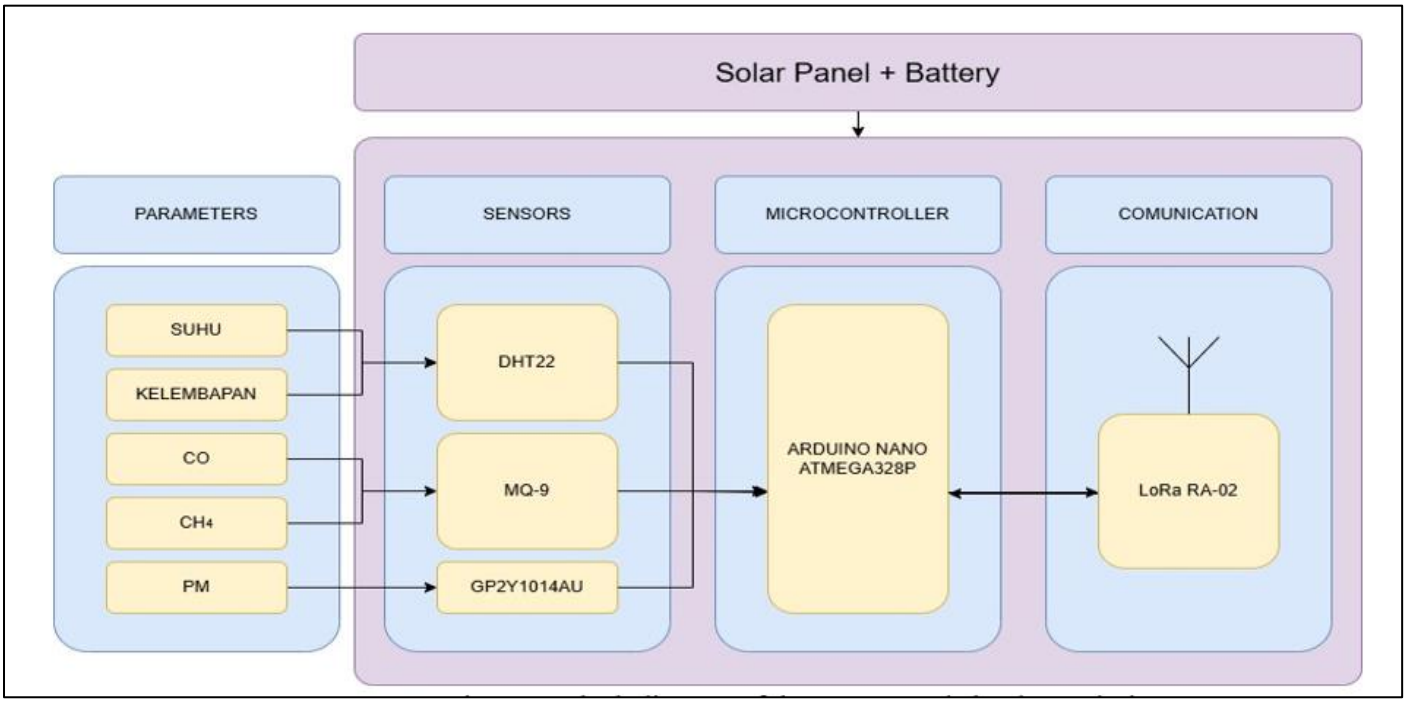

Fig 1: Block diagram of the Sensor Node hardware design

In the hardware design of the Sink Node, the focus is on communication. Not only does the Sink Node communicate with the Sensor Nodes, but it also communicates with the server so that the data obtained from the Sensor Nodes can be displayed on a website. To communicate with the server, the Sink Node uses ESP32 because it is integrated with WiFi module and serves as the microcontroller. To communicate with the Sensor Nodes, the Sink Node uses LoRa RA-02. To clarify the block diagram of the Sink Node hardware design, please refer to Figure 2.

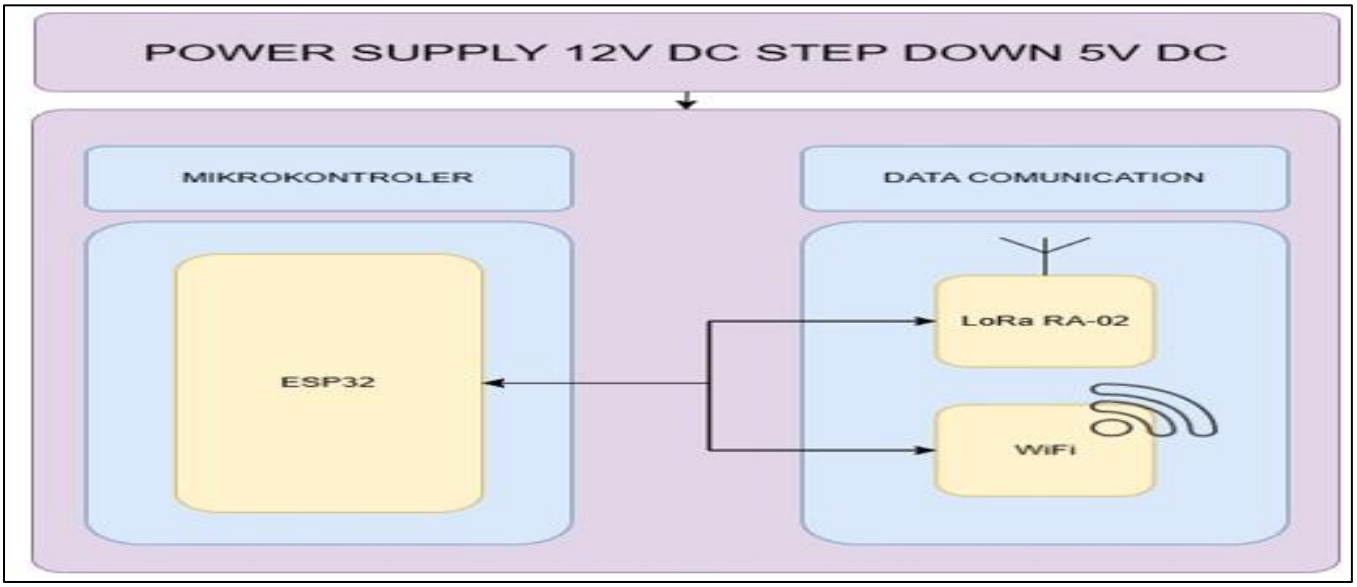

Fig 2: Block Diagram of the Sink Node Hardware Design

For the network architecture in this research, it is divided into two parts: the architecture for the Wireless Sensor Network and the architecture for the Internet of Things network. Both architectures work together to display data in real-time and allow access to the generated data by multiple users simultaneously using a website address.

The Wireless Sensor Network architecture in this research involves the Sink Node alternately requesting and receiving information from each connected Sensor Node using radio signals. The Sink Node then proceeds to transmit the data for users to view using the WiFi network. This is a simple approach to manage communication between one Sink Node and several Sensor Nodes in the network environment. For a clearer understanding, please refer to Figure 3.

ISSN No:-2456-2165 https://doi.org/10.38124/ijisrt/IJISRT24MAY1888

The network architecture of the Wireless Sensor Network in this research involves the Sink Node, which, upon receiving data, will transmit it using the WiFi network to the server. Subsequently, the data received by the Sink Node will be processed on the server so that it can be displayed to users via their smartphones or computers through a website page. For a clearer understanding, please refer to Figure 3.

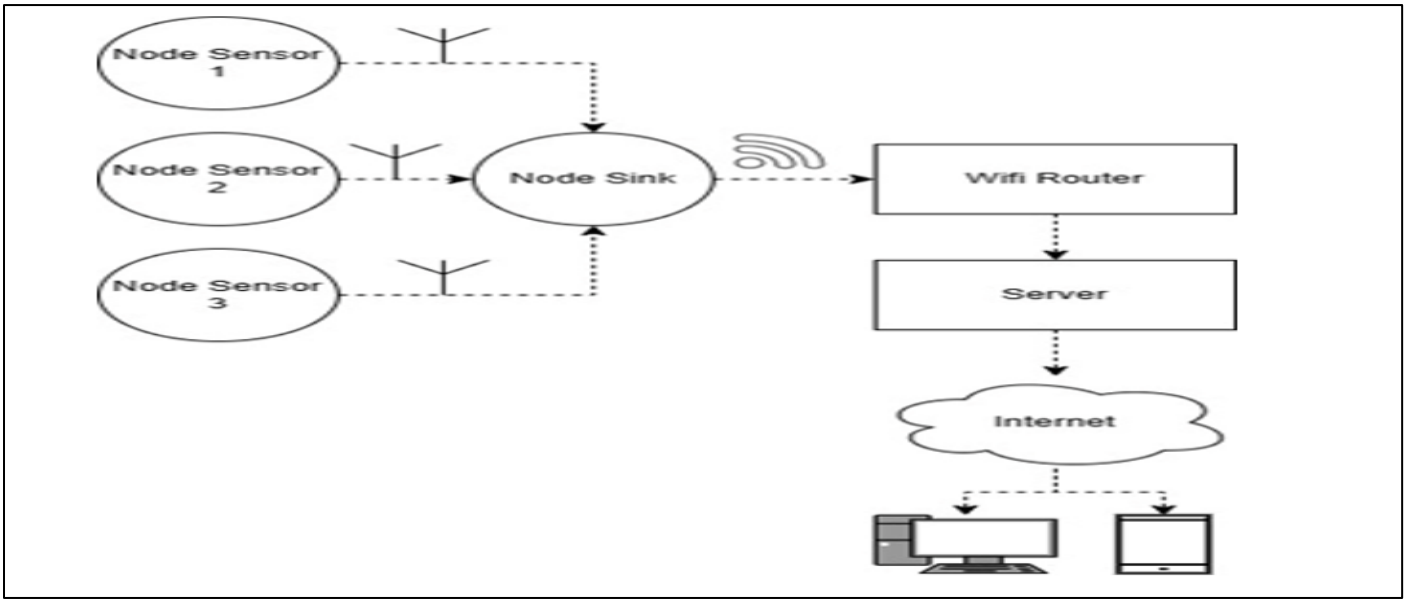

Fig 3: Flowchart of Measurement Results Display

III. RESULT AND DISCUSION

A. Device Description

The designed device is a Wireless Sensor Network (WSN) and Internet of Things (IoT) based system specifically designed to monitor air quality in a particular environment. This system consists of several sensors installed at specified locations, capable of measuring various air quality parameters, including CO, temperature, and humidity. The device comprises several hardware components: 3 Sensor Nodes and 1 Sink Node. Additionally, the device is equipped with a web-based interface that allows users to monitor air quality in real-time and view historical data. The Sink Node device can be seen in Figure 4.

Fig 4: Node Sensor

B. Kalibrasi Sensor

The device characterization and calibration were conducted from May 6, 2024, to May 11, 2024. Characterization was performed at the Instrumentation Laboratory of the Physics Department, Universitas Diponegoro. Readings from sensors of Sensor Node 1 to Sensor Node 3 were compared with standard devices to determine linearity using

$$y = mx + c \quad (1)$$

$$m = \frac{N\sum xy - \sum x \sum y}{N\sum x^2 - (\sum x)^2} \quad (2)$$

$$c = \frac{\sum y - m\sum x}{N} \quad (3)$$

and coefficient of determination:

$$R^2 = 1 - \frac{SS_{res}}{SS_{tot}} \quad (4)$$

$$SS_{res} = \sum_{i=1}^{n}(y_i - \hat{y}_i)^2 \quad (5)$$

$$SS_{tot} = \sum_{i=1}^{n}(y_i - \bar{y})^2 \quad (6)$$

where y is the sensor output, x is the physical input, m is the slope of the line (sensitivity), c is the intercept (offset), and R^2 is a statistic that provides a measure of how well the linear regression line fits the data.

ISSN No:-2456-2165 https://doi.org/10.38124/ijisrt/IJISRT24MAY1888

The initial observation results for the temperature sensor at Sensor Node 1 yielded y = 1,0781x - 2,6019 with R^2 = 0,9956, at sensor node 2 y = 1,0763x - 2,5721 with R^2 = 0,995, and at sensor node 3 y = 1,0816x - 2,7673 with R^2 = 0,9948. The linear regression graphs of the initial observation results for the temperature sensor for Node 1 can be seen in Figure 5, for Node 2 can be seen In Figure 5, Node 1 is depicted. Node 2 can be observed in Figure 6, and Node 3 is shown in Figure 7.

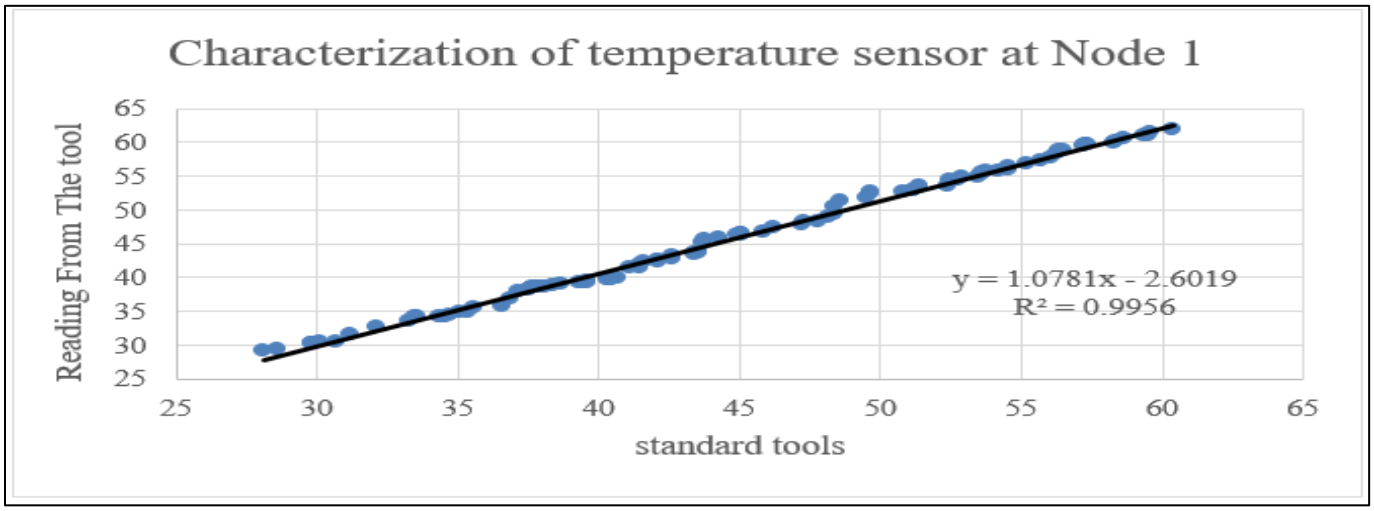

Fig 5: Characterization of Temperature Sensor at Node 1

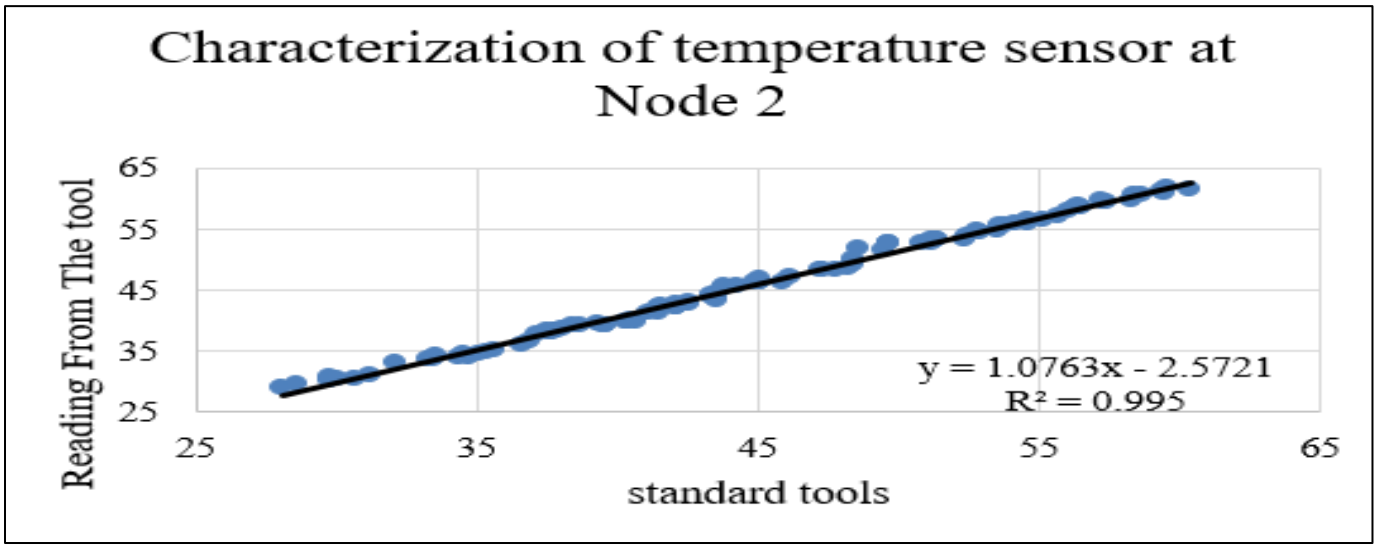

Fig 6: Characterization of Temperature Sensor at Node 2

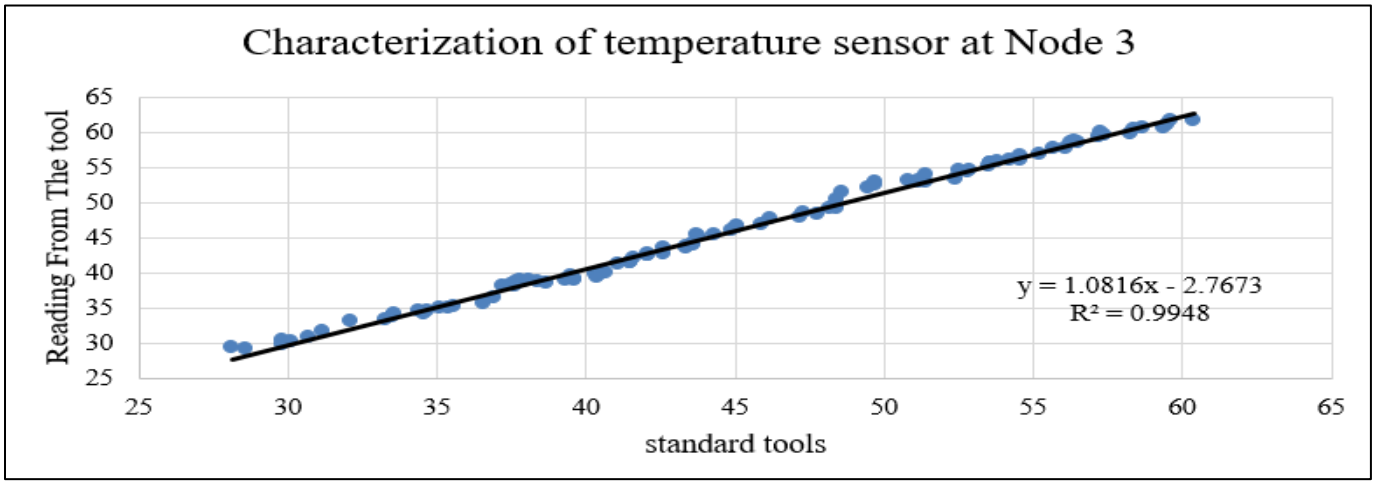

Fig 7: Characterization of Temperature Sensor at Node 3

ISSN No:-2456-2165 https://doi.org/10.38124/ijisrt/IJISRT24MAY1888

After inputting the linear equations into the program code, further observations were conducted. From the observations, the linear equations for the temperature sensor at Node 1 were found to be y = 0,997x + 0,1559 with R^2 = 0,9996, at node 2 y = 1,0021x - 0,0541 with R^2 = 0,9997, and at node 3 y = 1,001x - 0,0447 with R^2 = 0,9997. It can be seen that m approaches 1 and c approaches 0, proving that the calibrated temperature sensors exhibit close linearity to the standard devices. The linear regression graphs for Node 1 can be seen in Figure 8, for Node 2 in Figure 9, and for Node 3 in Figure 10.

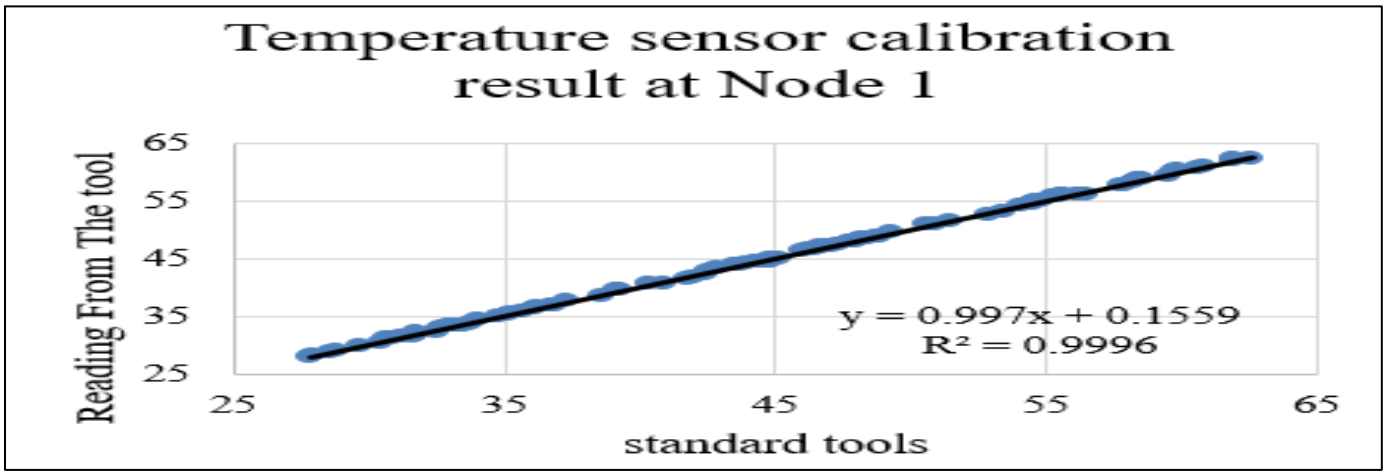

Fig 8: Temperature Sensor Calibration Result at Node 1

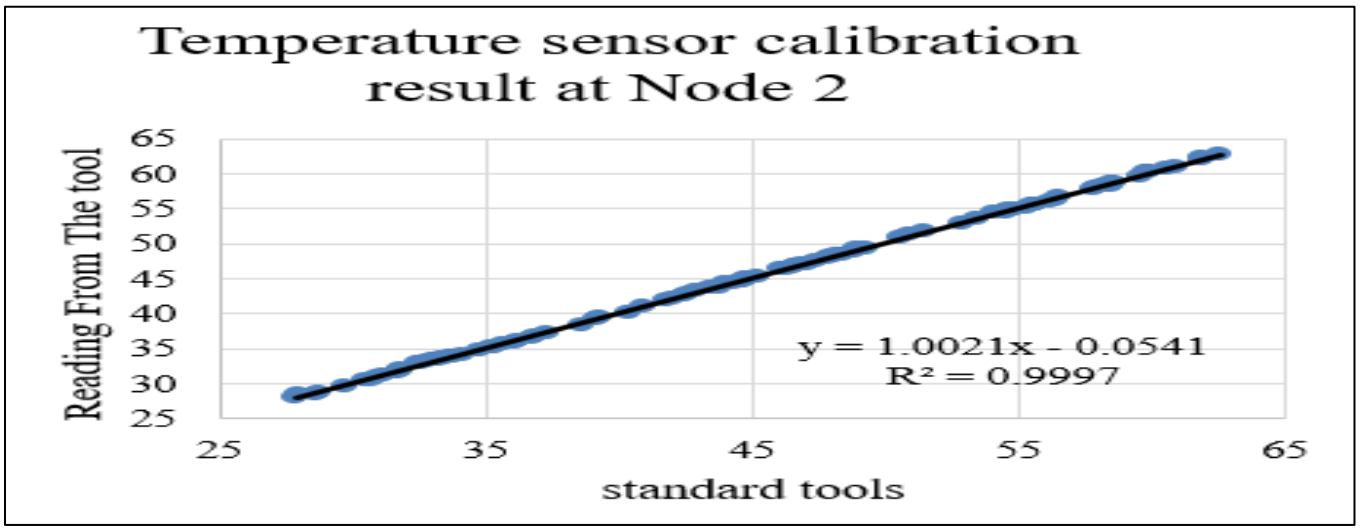

Fig 9: Temperature Sensor Calibration Result at Node 2

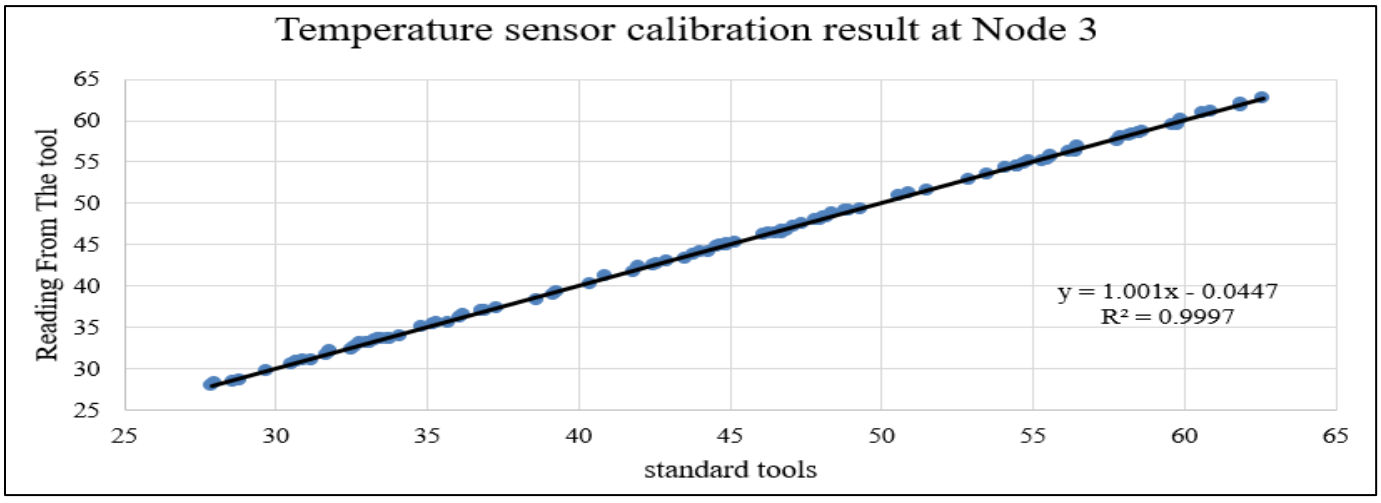

Fig 10: Temperature Sensor Calibration Result at Node 3

ISSN No:-2456-2165 https://doi.org/10.38124/ijisrt/IJISRT24MAY1888

The characterization of the humidity sensor at Sensor Node 1 to Sensor Node 3 was conducted by comparing the values from the DHT22 sensor with the standard device under the same conditions. The initial observation results for the humidity sensor at Sensor Node 1 yielded y = 1,0054x + 1,5415 with R^2 = 0,993, at sensor node 2 y = 1,0261x - 0,2041 with R^2 = 0,9928, and at sensor node 3 y = 1,0021x + 1,6186 with R^2 = 0,9941. The linear regression graphs of the initial observation results for the humidity sensor for Node 1 can be seen in Figure 11, for Node 2 in Figure 12, and for Node 3 in Figure 13.

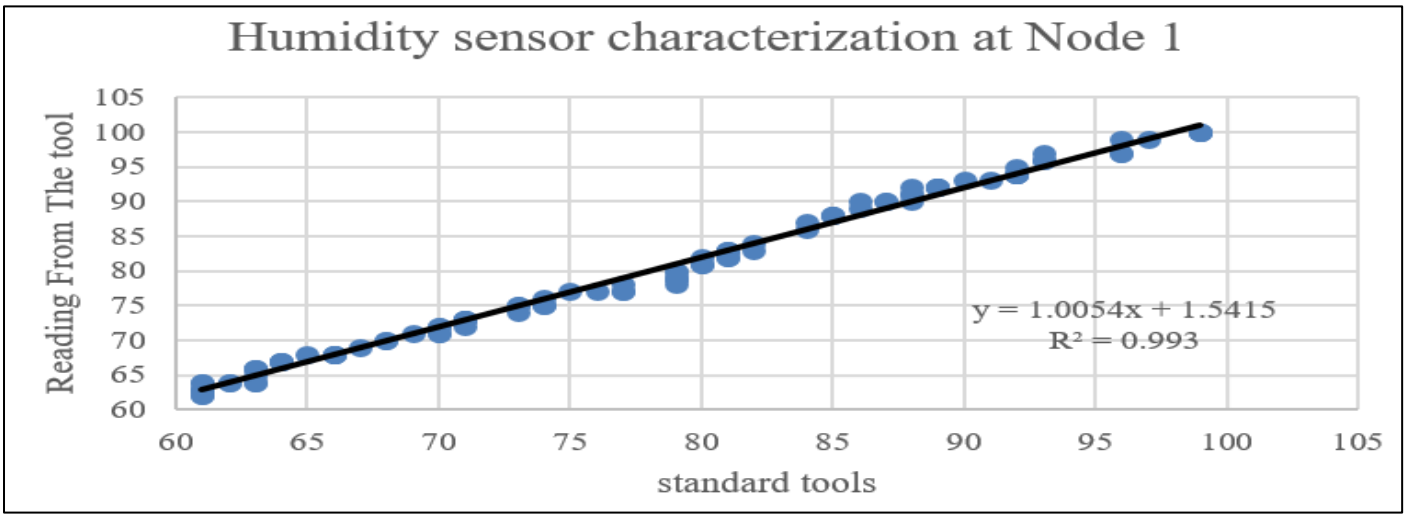

Fig 11: Humidity Sensor Characterization at Node 1

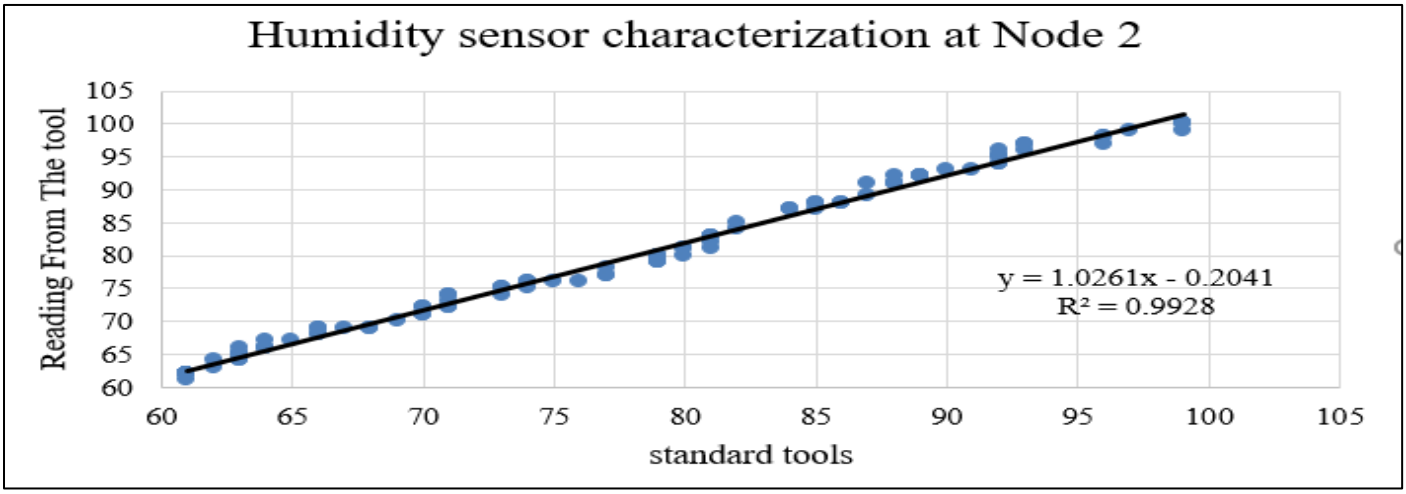

Fig 12: Humidity Sensor Characterization at Node 2

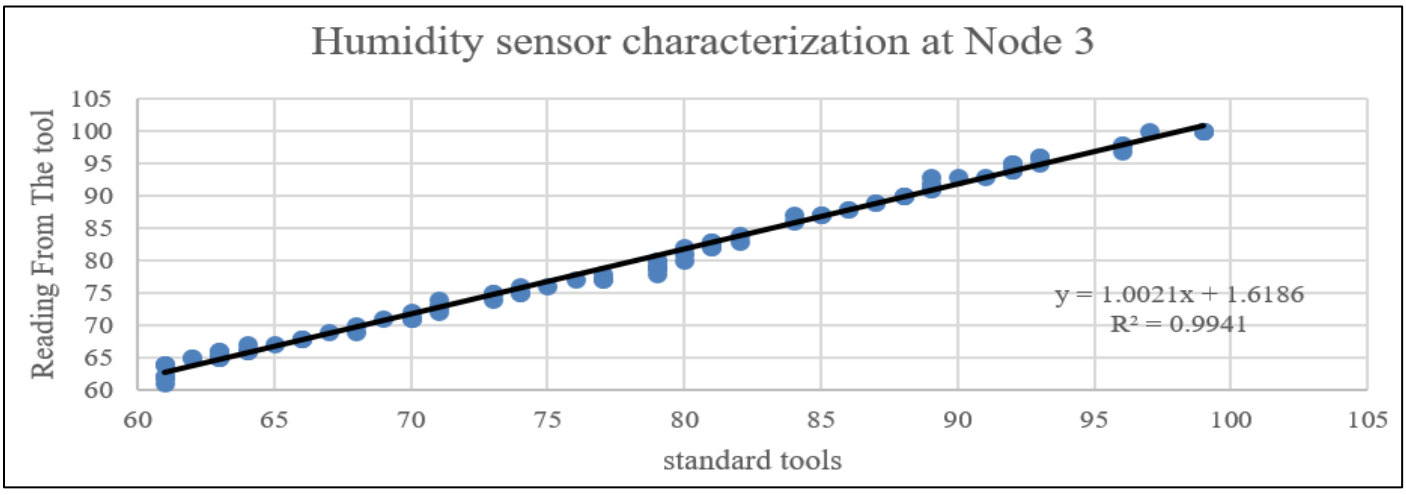

Fig 13: Humidity Sensor Characterization at Node 3

ISSN No:-2456-2165 https://doi.org/10.38124/ijisrt/IJISRT24MAY1888

After inputting the linear equations into the program code, further observations were conducted. From the observations, the linear equations for the humidity sensor at Node 1 were found to be y = 0,9966x + 0,221 with R^2 = 0,9969, at node 2 y = 1,0002x - 0,1526 with R^2 = 0,9975, and at node 3 y = 0,9968x + 0,3798 with R^2 = 0,9976. It can be seen that m approaches 1 and c approaches 0, proving that the calibrated humidity sensors exhibit close linearity to the standard devices. The linear regression graphs for Node 1 can be seen in Figure 14, for Node 2 in Figure 15, and for Node 3 in Figure 16.

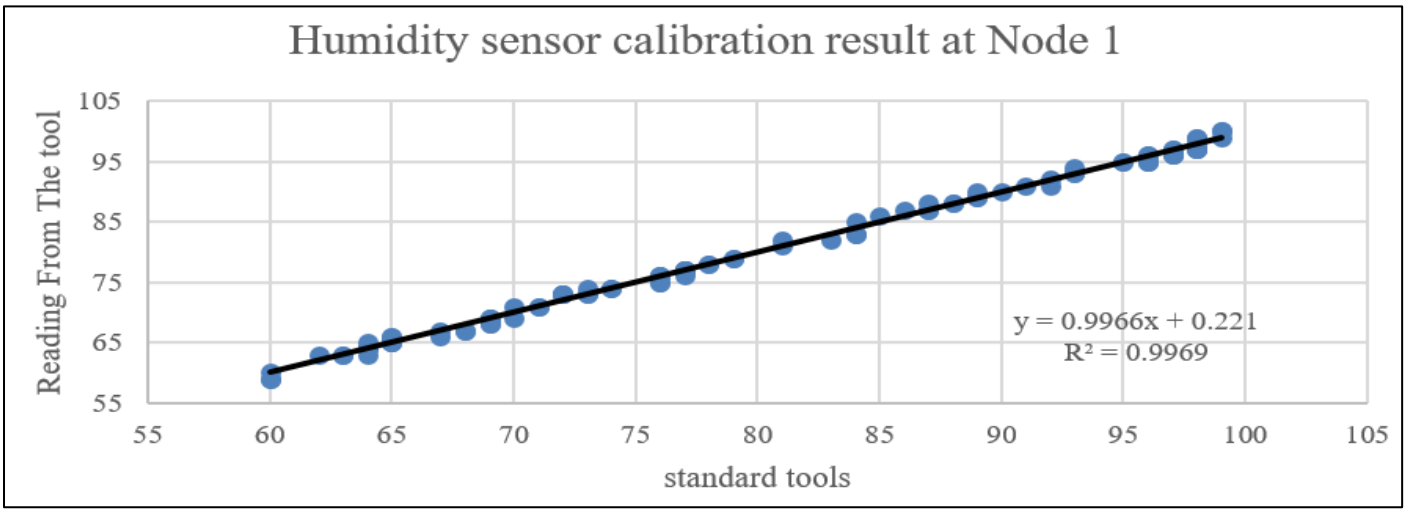

Fig 14: Humidity Sensor Calibration Result at Node 1

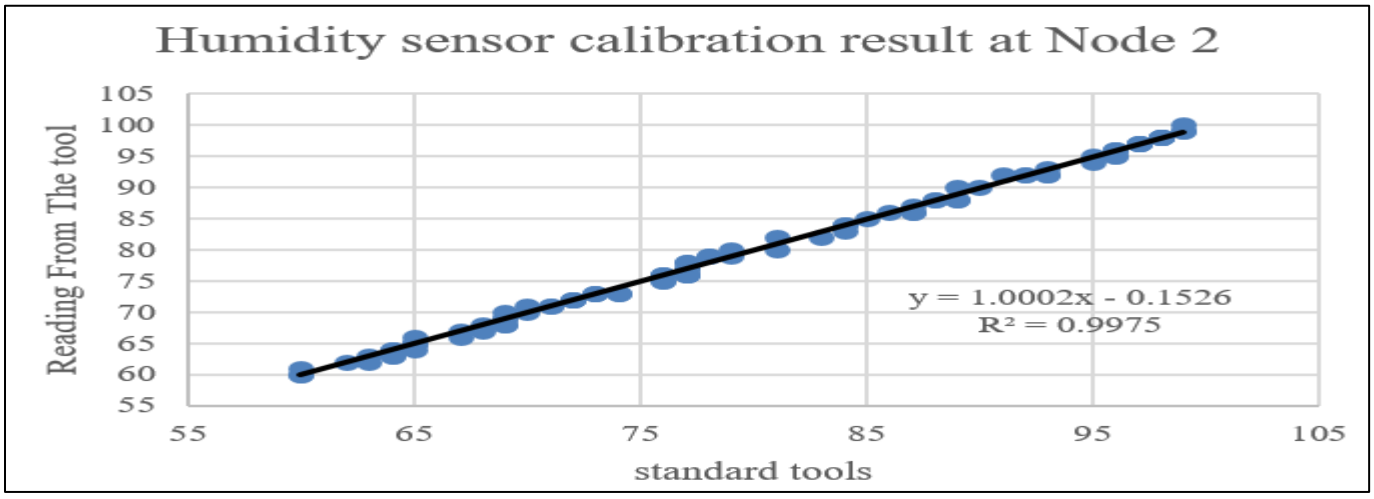

Fig 15: Humidity Sensor Calibration Result at Node 2

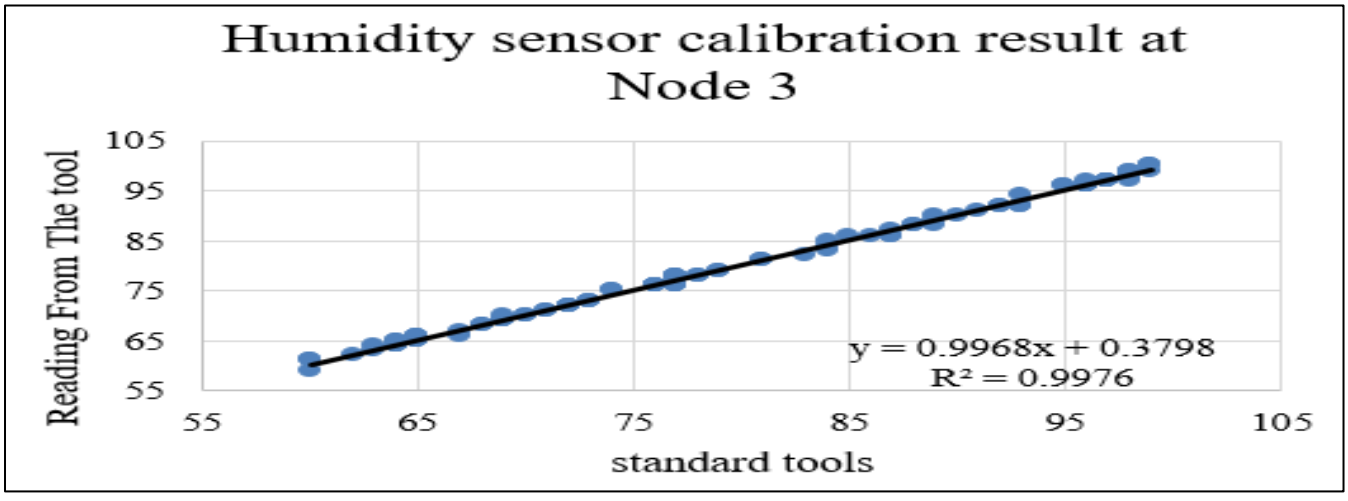

Fig 16: Humidity Sensor Calibration Result at Node 3

ISSN No:-2456-2165 https://doi.org/10.38124/ijisrt/IJISRT24MAY1888

The characterization of the CO sensor at Sensor Node 1 to Sensor Node 3 was conducted by comparing the values from the MQ-9 sensor with the standard device under the same conditions. The initial observation results for the CO sensor at Sensor Node 1 yielded y = 0,8499x + 28,018 with R^2 = 0,9968, at sensor node 2 y = 0,85x + 28,631 with R^2 = 0,9965, and at sensor node 3 y = 0,8496x + 28,337 with R^2 = 0,9966. The linear regression graphs of the initial observation results for the CO sensor for Node 1 can be seen in Figure 17, for Node 2 in Figure 18, and for Node 3 in Figure 19.

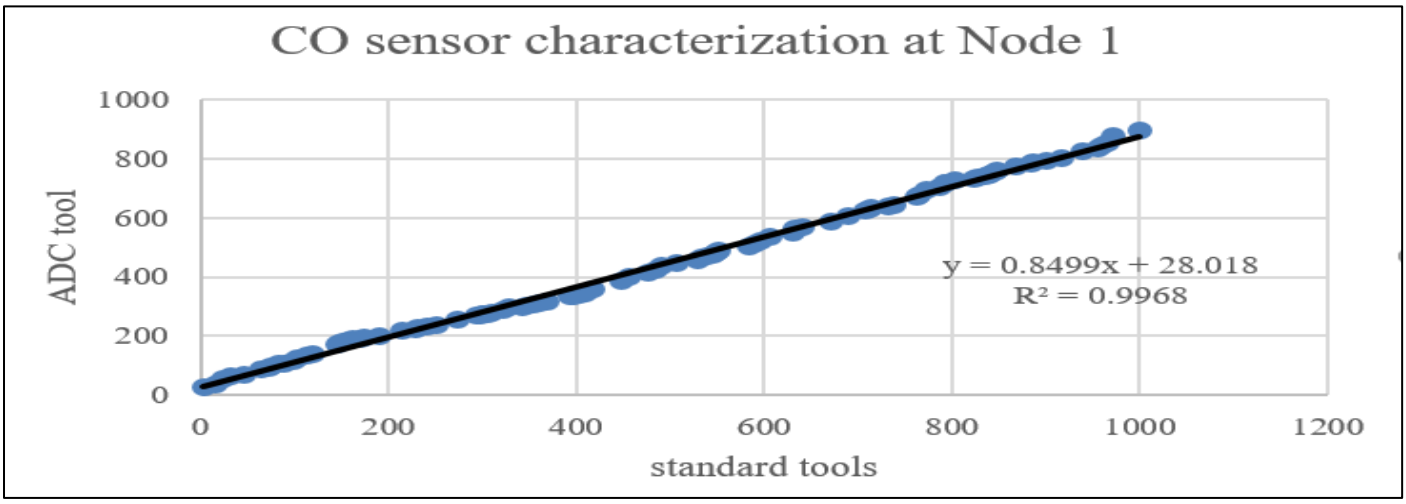

Fig 17: CO Sensor Characterization at Node 1

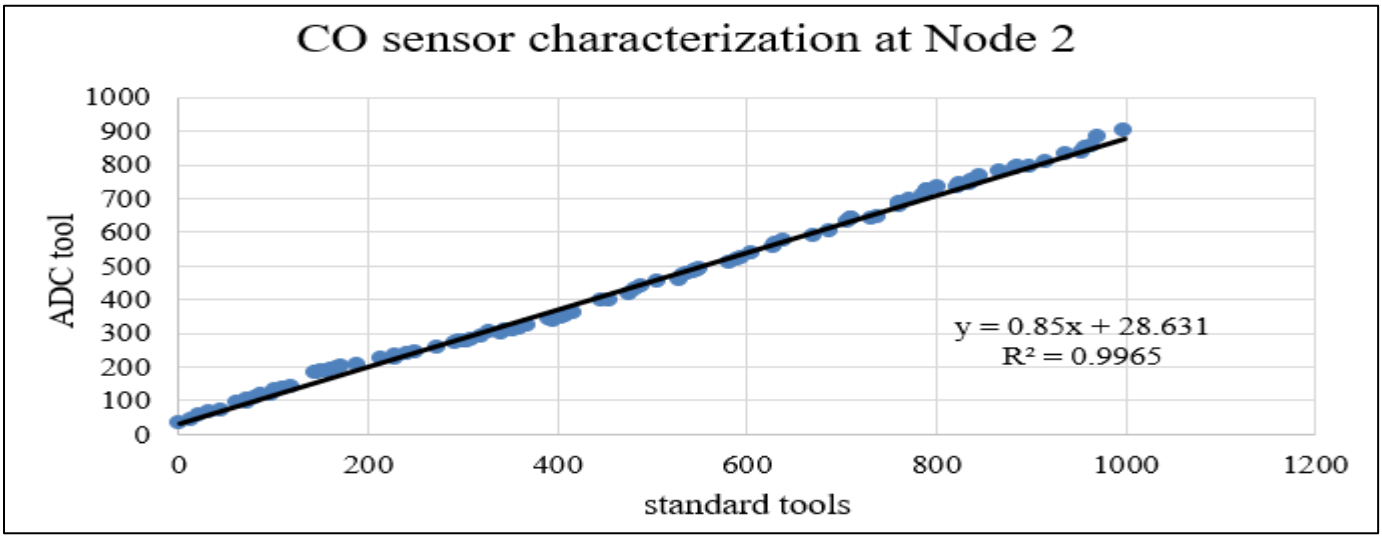

Fig 18: CO Sensor Characterization at Node 2

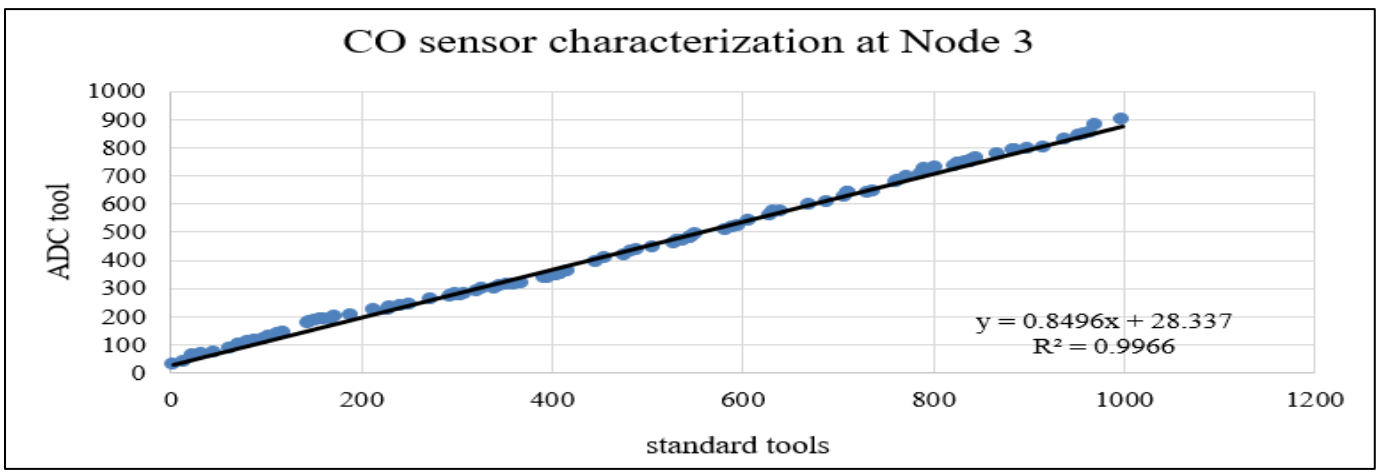

Fig 19: CO Sensor Characterization at Node 3

ISSN No:-2456-2165 https://doi.org/10.38124/ijisrt/IJISRT24MAY1888

After inputting the linear equations into the program code, further observations were conducted. From the observations, the linear equations for the CO sensor at Node 1 were found to be y = 1,0125x - 2,8285 with R^2 = 0,9997, at node 2 y = 1,0128x - 3,028 with R^2 = 0,9997, and at node 3 y = 1,0117x - 1,6228 with R^2 = 0,9997. It can be seen that m approaches 1 and c approaches 0, proving that the calibrated CO sensors exhibit close linearity to the standard devices. The linear regression graphs for Node 1 can be seen in Figure 20, for Node 2 in Figure 21, and for Node 3 in Figure 22.

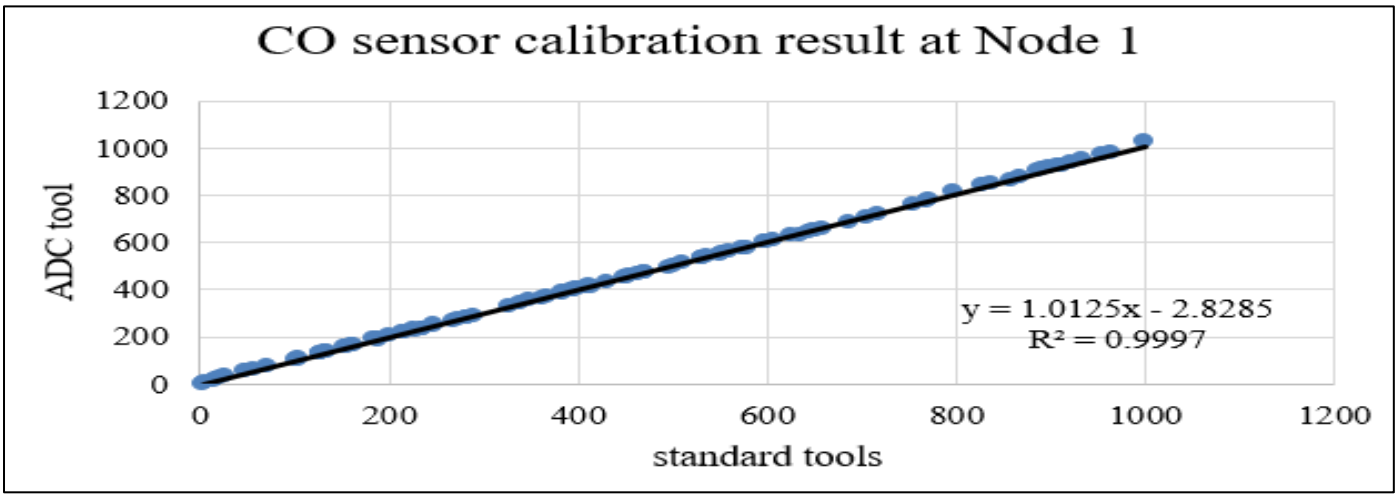

Fig 20: CO Sensor Calibration Result at Node 1

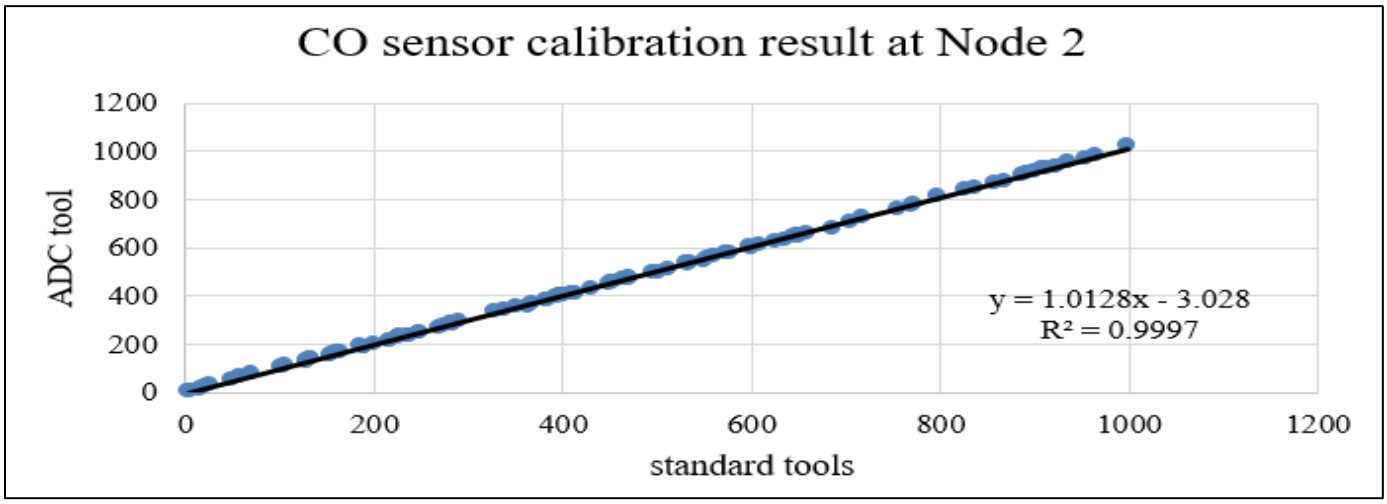

Fig 21: CO Sensor Calibration Result at Node 2

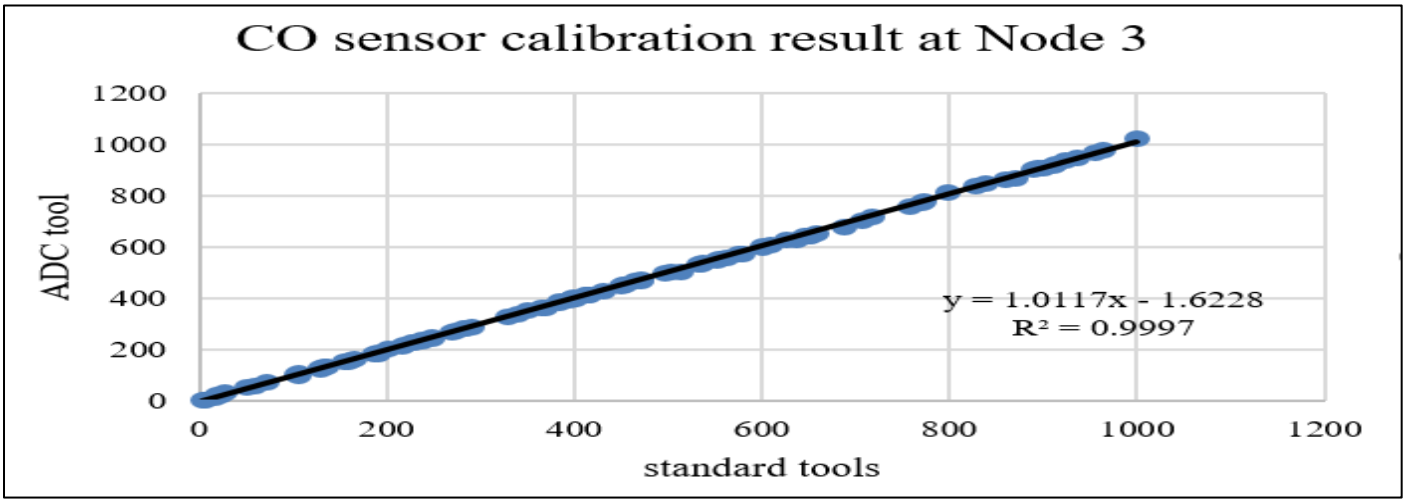

Fig 22: CO Sensor Calibration Result at Node 3

ISSN No:-2456-2165 https://doi.org/10.38124/ijisrt/IJISRT24MAY1888

The CO sensor readings from Sensor Node 1 to Sensor Node 3 were compared with AQMS to determine the standard deviation using the formulas:

$$s_x^2 = \frac{\sum(x_i - \bar{x})^2}{N} \quad (7)$$

$$s_y^2 = \frac{\sum(y_i - \bar{y})^2}{N} \quad (8)$$

Then, the Mean Absolute Percentage Error (MAPE) of the obtained data was calculated using the formula:

$$MAPE = \frac{1}{n}\sum_{i=1}^{n}\left|\frac{y_i - \widehat{y_i}}{y_i}\right| . 100\% \quad (9)$$

Next, to assess the coefficient of determination using formula (4) and perform calibration using the linearity calibration formula (1). Before converting to the ISPU unit, the unit of the device, ppm, is converted to the unit $\mu g/m^3$ first using the formula:

$$\frac{\mu g}{m^3} = ppm. 1000 \frac{MW}{24,45} \quad (10)$$

Where MW CO = 28,01

Finally, the ISPU unit was obtained using the formula:

$$I = \frac{(I_a - I_b)}{(X_a - X_b)}(X_X - X_b) + I_b \quad (11)$$

And presented in Table 1.

Table 1: Conversion of ISPU Parameter Values

ISPU	24 Jam partikulat (PM_{10}) µg/m³	24 Jam partikulat ($PM_{2.5}$) µg/m³	24 Jam sulfur dioksida (SO_2) µg/m3	24 Jam karbon monoksida (CO) µg/m³	24 Jam ozon (O_3) µg/m³	24 jam nitrogen dioksida (NO_2) µg/m³	24 Jam hidrokarbon (HC) µg/m³
0 - 50	50	15,5	52	4000	120	80	45
51 - 100	150	55,4	180	8000	235	200	100
101 - 200	350	150,4	400	15000	400	1130	215
201 - 300	420	250,4	800	30000	800	2260	432
>300	500	500	1200	45000	1000	3000	648

After applying the formulas into the code program, the sensor readings are now in ISPU units. The initial observations for the CO sensor at node sensor 1 yielded s = 1,68, y = 0,7693x + 1,824, R^2 = 0,8902 with MAPE = 4,95%, at sensor node 2 s = 1,64, y = 0,794x + 1,7619, R^2 = 0,9009 with MAPE = 5,09% and at sensor node 3 s = 1,52, y = 0,8456x + 1,1895, R^2 = 0,8759 with MAPE = 3,88% For the standard deviation of the data obtained from AQMS s = 1,37. The linear regression graphs of the initial observations for CO sensor at node 1 can be seen in Figure 23, node 2 in Figure 24, and node 3 in Figure 25.

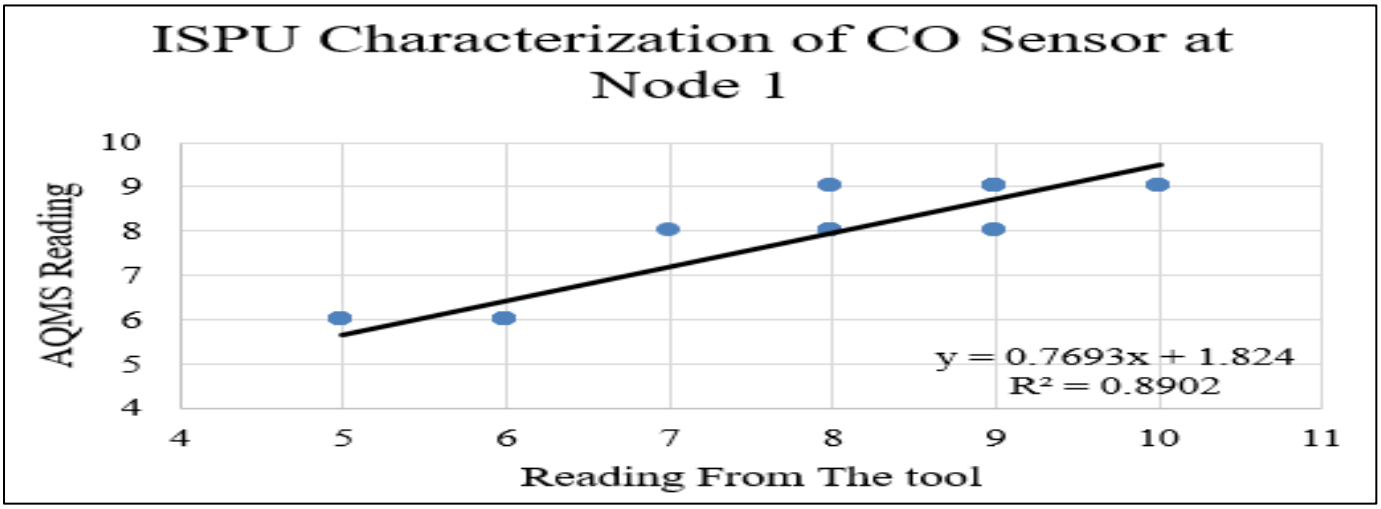

Fig 23: ISPU Characterization of CO Sensor at Node 1

ISSN No:-2456-2165 https://doi.org/10.38124/ijisrt/IJISRT24MAY1888

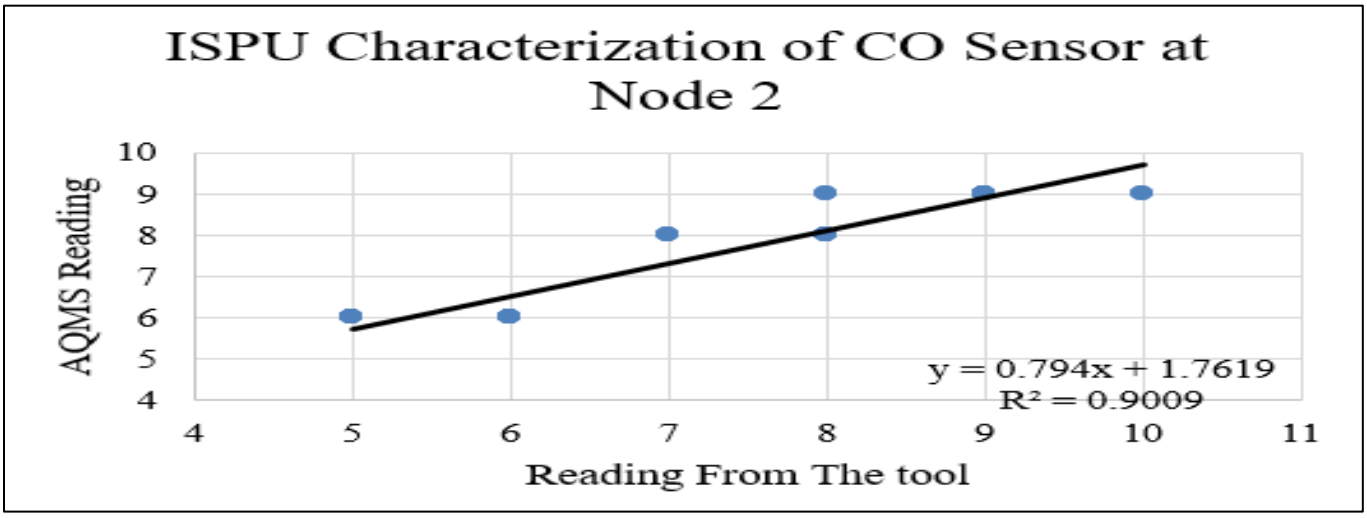

Fig 24: ISPU Characterization of CO Sensor at Node 2

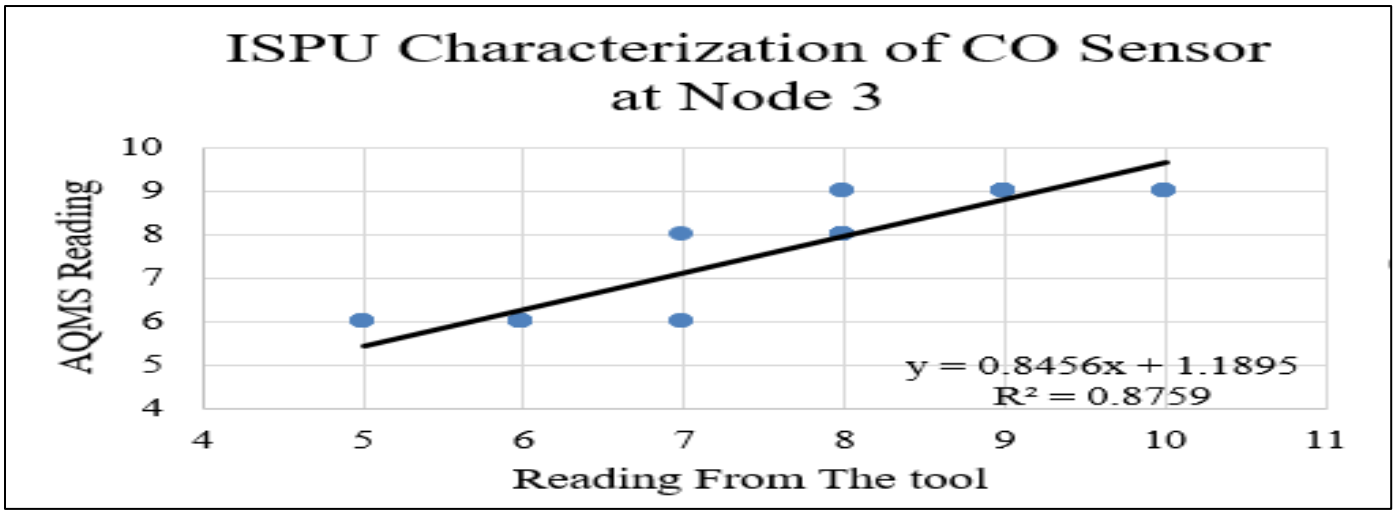

Fig 25: ISPU Characterization of CO Sensor at Node 3

The system was tested in the Faculty of Science and Mathematics, Universitas Diponegoro, as depicted in Figure 26, where the blue nodes represent sensor nodes and the red one represents the sink node. The distances between sensor nodes and the sink node are approximately ±110 m for node 1, ±20 m for node 2, and ±100 m for node 3, showing good average air quality results as seen in Figures 27, 28, and 29.

Fig 26: Location of Sensor Nodes and Sink Node

ISSN No:-2456-2165 https://doi.org/10.38124/ijisrt/IJISRT24MAY1888

Fig 27: Real-Time CO Graph

Fig 28: Real-Time Humidity Graph

Fig 29: Real-Time Temperature Graph

ISSN No:-2456-2165 https://doi.org/10.38124/ijisrt/IJISRT24MAY1888

IV. CONCLUSIONS

➢ *Based on the Testing and Analysis Conducted, it can be Concluded That:*

- The device capable of simultaneously monitoring multiple air quality parameters, including temperature, humidity, and CO concentration, has been successfully designed and can function well.
- Successfully integrated the Wireless Sensor Network and Internet of Things system with 3 sensor nodes and 1 Sink Node to collect air quality data from different locations simultaneously, integrated with solar panels as the power source.
- Able to display measurement data in real-time via the internet, accessible at pillarsensors.my.id, allowing real-time monitoring and data analysis through graphical representations.

ACKNOWLEDGMENT

We would like to express our gratitude to the Physics Study Program, Universitas Diponegoro, for providing the necessary facilities and equipment for this experiment. We also want to thank the technical teams of DLH Ungaran and DLH Kota Semarang for their assistance in data collection and sensor calibration. Finally, we thank our families and friends for their continuous support and encouragement throughout this project.

REFERENCES

[1]. Fotopoulou, E., Zafeiropoulos, A., PAPASPYROS, D., HASAPIS, P., TSIOLIS, G., BOURAS, T., MOUZAKITIS, S., & Zanetti, N. (2016). Linked data analytics in interdisciplinary studies:The health impact of air pollution in urban areas. IEEE Access 4, 149–164.

[2]. Cabaneros, S., M., Calautit, J., K., Hughes, B. R. (2019). A review of artificial neural network models for ambient air pollution prediction, Environmental Modelling & Software, Volume 119, Pages 285-304, ISSN 1364-8152.

[3]. Shaban, K., B., Kadri, A., Rezk, E. (2016). Urban air pollution monitor-ing system with forecasting models. IEEE Sensor, 16 (8), 2598–2606.

[4]. Li, W., Y., Lo, K., M., Mak, T., Leung, K., S., Leung, Y., Meng, M., L. (2015). A Survey of wireless sensor networkbased air pollution monitoring systems. Sensors, 15(12), 31392–31427.

[5]. William, P., Kiran, Y., V., U., Rana, A., Gangodkar, D., Khan, I., Ashutosh, K., (2022). Design and implementation of IoT based framework for air quality sensing and monitoring. in: 2022 2nd International Conference on Technological Advancements in Computational Sciences (ICTACS), 197–200.

[6]. Sinha, S., Makkar, P. (2021). In Advances in ubiquitous sensing applications for healthcare. Security and Privacy Issues in IoT Devices and Sensor Networks,Academic Press, Pages 1-27, ISSN 25891014, ISBN 9780128212554.

[7]. Singh, S., Singh, U. (2022). The effect of chaotic mapping on naked mole-rat algorithm for energy efficient smart city wireless sensor network. Computers & Industrial Engineering, 173(1), pp 1-19.

[8]. Liu, J., Sui, X. (2021). Hospital wireless sensor network coverage and ambroxol hydrochloride in the treatment of mycoplasma pneumonia in children. Microprocessors and Microsystems, 81(1), 103707-103712.

[9]. Sharma, N., Gupta, V. (2022). A Framework for Wireless Sensor Network Optimization Using Fuzzy-Based Fractal Clustering to Enhance Energy Efficiency. Journal of Circuits, Systems and Computers, 34(13), 29-54.

[10]. Laksmana, I., Jingga, T., Z., Febrina,, W., Khomarudin, A., N., Putri, E., E., Novita, R., N., R., Amrizal, 2022, teknologi internet of things (iot) dan hidroponik, Goresan Pena, isbn 9786233674683.

[11]. Juliando, D., E., Putra, R., Sartika, D., A., Yudha, R., G., P. (2021). Study of Lora Module Ra-02 For Long Range, Low Power, LowRate Picture Transfer Applications. Journal of Physics Conference Series, 1845(1).

[12]. Jacobson, M., Z., & Delucchi, M., A. (2011). Providing all global energy with wind, water, and solar power, Part I: Technologies, energy resources, quantities and areas of infrastructure, and materials. Energy Policy, 39(3), 1154-1169.

[13]. Barbose, G., Darghouth, N., & Millstein, D. (2017). The impact of rate design and net metering on the bill savings from distributed PV for residential customers in California. Energy Policy, 105, 385-394.

[14]. Salman, N., Andrew, Kemp, H., Khan, A., & Noakes, C., J. (2019). Real Time Wireless Sensor Network (WSN) based Indoor Air Quality Monitoring System. IFAC-PapersOnLine, 52(24), 324-327.